

Cascade production in heavy-ion collisions at SIS energies

Lie-Wen Chen,^{1,*} Che Ming Ko,¹ and Yiharn Tzeng²

¹*Cyclotron Institute and Physics Department,
Texas A&M University, College Station, Texas 77843-3366*

²*Institute of Physics, Academia Sinica, Taipei 11529, Taiwan*

(Dated: December 30, 2021)

Abstract

Production of the doubly strange Ξ baryon in heavy-ion collisions at SIS energies is studied in a relativistic transport model that includes perturbatively the strangeness-exchange reactions $\bar{K}\Lambda \rightarrow \pi\Xi$ and $\bar{K}\Sigma \rightarrow \pi\Xi$. Taking the cross sections for these reactions from the predictions of a hadronic model, we find that the Ξ yield is about 10^{-4} in central collisions of $^{58}\text{Ni} + ^{58}\text{Ni}$ at $E/A = 1.93$ GeV. The Ξ yield is further found to be more sensitive to the magnitude of the cross sections for strangeness-exchange reactions than to the medium effects due to modified kaon properties. We have also made predictions for Ξ production in Au+Au collisions at energies from 1 to 2 GeV/nucleon.

PACS numbers: 25.75.-q

*On leave from Department of Physics, Shanghai Jiao Tong University, Shanghai 200030, China

I. INTRODUCTION

Production of the doubly strange baryon Ξ has been studied in heavy ion collisions at various energies. For ultrarelativistic energies at SPS, the measured Ξ abundance is significantly enhanced compared to that expected from initial nucleon-nucleon collisions [1]. Explanations for this enhancement include exotic mechanisms due to the formation of the quark-gluon plasma, topological defects, and color ropes as well as more conventional processes of strangeness-exchange reactions such as $\bar{K}\Lambda \rightarrow \pi\Xi$ and $\bar{K}\Sigma \rightarrow \pi\Xi$ [2]. In the latter case, the experimental data can, however, only be explained if a relatively high dense hadronic matter exists in these collisions. Observations of Ξ production at lower energies at the AGS, e.g., Au+Au collisions at 6 AGeV [3], have also been reported recently, and the measured yield is comparable to the predictions from the transport model based on strangeness-exchange reactions [4]. Again, the hadronic density reached in these collisions is quite large with maximum density reaching 7-8 times normal nuclear matter density. In all these cases, the Ξ yield seems to be consistent with that given by the statistical model [5]. Although both \bar{K} and $\Lambda(\Sigma)$ are infrequently produced in heavy ion collisions at lower GSI energies, i.e., about 1-2 AGeV, which are below the threshold for producing these particles from nucleon-nucleon collisions in free space, studies of their production have provided valuable information about the nuclear equation of state at high densities as well as the in-medium properties of hadrons [6, 7]. The latter is believed to be related to the partial restoration of chiral symmetry in hot dense matter.

In the present study, Ξ production in heavy-ion collisions at SIS energies, which are below the threshold of about 3.7 GeV for its production in nucleon-nucleon collisions in free space is studied in the framework of a relativistic transport model. We include Ξ production from the strangeness-exchange reactions $\bar{K}\Lambda \leftrightarrow \pi\Xi$ and $\bar{K}\Sigma \leftrightarrow \pi\Xi$ with their cross sections taken from the predictions of a coupled-channel approach based on a flavor SU(3)-invariant hadronic Lagrangian [8]. The Ξ yield from these collisions thus depends on the cross sections for these reactions as well as the abundance of \bar{K} , Λ and Σ in the collisions. Medium effects due to modified kaon properties are also studied as it is known to affect the production of \bar{K} , Λ , and Σ in dense matter [6, 7, 9, 10, 11, 12]. We find that the final Ξ yield is not much affected by the medium effects but is sensitive to the cross sections for the strangeness-exchange reactions, thus offering the possibility of testing the predicted cross sections from

the hadronic model.

II. THE RELATIVISTIC TRANSPORT MODEL

The transport model used in present study is taken from that of Refs. [11, 12] based on the relativistic Vlasov-Uehling-Uhlenbeck equation (RVUU) [13]. In this model, only the nucleon, delta resonance, and pion are treated explicitly. Besides undergoing elastic and inelastic two-body scatterings, these particles also propagate in mean-field potentials. For nucleons, their potential is taken from the effective chiral Lagrangian of Ref.[14] instead of the nonlinear Walecka model used in Ref.[13]. As a result, their motions are given by the Hamilton equation of motion,

$$\frac{d\mathbf{x}}{dt} = \frac{\mathbf{p}^*}{E^*}, \quad \frac{d\mathbf{p}}{dt} = -\nabla_x(E^* + W_0). \quad (1)$$

where $E^* = \sqrt{\mathbf{p}^{*2} + m^{*2}}$ with $\mathbf{p}^* = \mathbf{p} - \mathbf{W}$ and $m^* = m - \Phi$, and Φ and $W = (W_0, \mathbf{W})$ are the scalar and vector mean-field potentials. For mean-field parameters, we use the set T1 that gives a nuclear matter incompressibility $K_0 = 194$ MeV and a nucleon effective mass $m^*/m = 0.60$ at normal nuclear matter density $\rho_0 = 0.15 \text{ fm}^{-3}$. The Δ resonance is assumed to have the same mean-field potential as the nucleon, while the mean-field potential for the pion is neglected.

Kaons together with its partners (hyperons or antikaons) are produced in this model from pion-baryon and baryon-baryon reactions, i.e., $\pi B \rightarrow KY$ and $BB \rightarrow BYK$. In Refs.[11, 12], the cross section for the reaction $\pi B \rightarrow KY$ is taken from the resonance model of Ref.[15]. Here, we use that from an improved resonance model [16]. The cross section for the reaction $BB \rightarrow BYK$ is, on the other hand, taken from the one-boson-exchange model of Refs. [17, 18]. Antikaons in this model are produced not only from pion-baryon and baryon-baryon reactions, i.e., $\pi B \rightarrow K\bar{K}B$ and $BB \rightarrow BBK\bar{K}$, but also from the pion-hyperon reactions $\pi Y \rightarrow \bar{K}N$ [19], where Y denotes either Λ or Σ . Their cross sections are taken either from predictions of the boson-exchange model or from the empirical values as in Ref. [11]. Annihilation of produced antikaons is included via the inverse reactions of pion-hyperon reactions, i.e., $\bar{K}N \rightarrow \pi Y$, as other absorption reactions involve the rarely produced kaons and are thus unimportant. However, the annihilation of kaons is neglected as it has little effect on kaon production [20]. Because of the small production probabilities

of kaons, hyperons, and antikaons in heavy-ion collisions at SIS energies, the above discussed reactions are treated perturbatively. In this method, the dynamics of nucleons, Δ resonances, and pions that produce these particles are not affected, and the produced particle is given a probability determined by the ratio of its production cross section to the total two-body scattering cross section.

After being produced, these rare particles also undergo elastic and inelastic scattering as well as propagate in mean-field potentials. For Λ and Σ , their mean-field potentials are taken to be 2/3 of the nucleon potential according to their light quark content. For kaon and antikaon, their mean-field potentials are obtained from the chiral Lagrange including both scalar and vector interactions [11], i.e.,

$$\omega_{K,\bar{K}} = \left[m_K^2 + \mathbf{k}^2 - a_K \rho_S + (b_K \rho)^2 \right]^{1/2} \pm b_K \rho. \quad (2)$$

In the above, we have $b_K = 3/(8f_\pi^2) \approx 0.333 \text{ GeVfm}^3$ corresponding to a pion decay constant $f_\pi \approx 103 \text{ MeV}$; ρ and ρ_s are, respectively, the nuclear matter and scalar density; and the “+” and “−” signs in the last term are for kaon and antikaon, respectively. The two parameters a_K and $a_{\bar{K}}$, which determine the strength of the attractive scalar potential for kaon and antikaon, respectively, can in principle be evaluated from the chiral Lagrangian [21]. Here, we follow the method of Ref.[11] by determining their values from fitting the experimental data on kaon and antikaon yield in heavy-ion collisions using the RVUU model, and this will be described in detail later.

The perturbative method for rare particle production in heavy ion collisions was first introduced in Ref.[22] and is now extensively used in transport models [6, 7]. Since the yield of Ξ particle is expected to be small at SIS energies, it is treated perturbatively as well. The produced Ξ from the strangeness-exchange reactions $\bar{K}Y \rightarrow \pi\Xi$ is thus given a probability equal to the ratio of this cross section to the $\bar{K}Y$ total cross section, which is taken to be 20 mb, multiplied by the probabilities carried by \bar{K} and Y . Since the final Ξ yield is given by the product of its production probability in the reaction $\bar{K}Y \rightarrow \pi\Xi$ and the number of $\bar{K}Y$ collisions, which is proportional to the $\bar{K}Y$ total cross section, it depends only on the cross section for the reaction $\bar{K}Y \rightarrow \pi\Xi$ but not on the $\bar{K}Y$ total cross section. During its propagation in the nuclear medium, the Ξ is subjected to a mean-field potential that is 1/3 of the nucleon potential as it has only one light quark.

III. THE STRANGENESS-EXCHANGE REACTIONS $\bar{K}\Lambda \rightarrow \pi\Xi$ AND $\bar{K}\Sigma \rightarrow \pi\Xi$

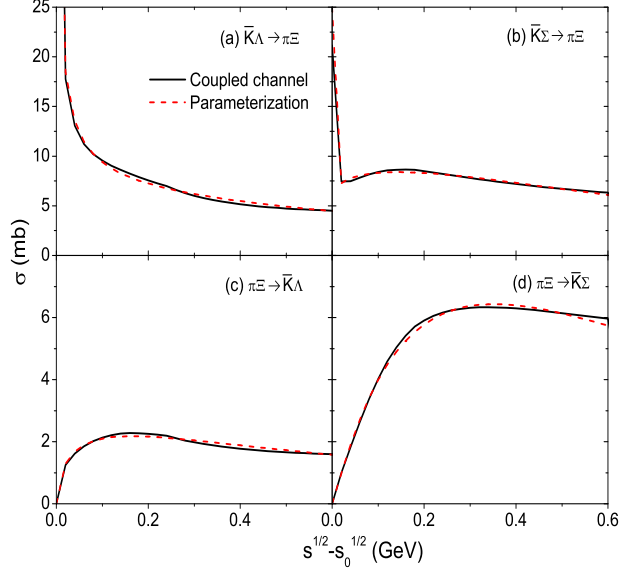


FIG. 1: Isospin-averaged cross sections for (a) $\bar{K}\Lambda \rightarrow \pi\Xi$, (b) $\bar{K}\Sigma \rightarrow \pi\Xi$, (c) $\pi\Xi \rightarrow \bar{K}\Lambda$, and (d) $\pi\Xi \rightarrow \bar{K}\Sigma$. Solid curves are from the coupled-channel calculations of Ref. [8] with a cutoff parameter of 1 GeV, and dashed curves are parameterized ones based on Eq.(4).

For the strange-exchange reactions $\bar{K}Y \rightarrow \pi\Xi$, there is no empirical information on their cross sections. These reactions have, however, been studied in the coupled-channel approach based on a gauged flavor SU(3)-invariant hadronic Lagrangian [8]. The spin- and isospin-averaged cross sections for these reactions can be written as

$$\sigma_{\bar{K}\Lambda \rightarrow \pi\Xi} = \frac{1}{4} \frac{p_\pi}{p_{\bar{K}}} |M_{\bar{K}\Lambda \rightarrow \pi\Xi}|^2, \quad \sigma_{\bar{K}\Sigma \rightarrow \pi\Xi} = \frac{1}{12} \frac{p_\pi}{p_{\bar{K}}} |M_{\bar{K}\Sigma \rightarrow \pi\Xi}|^2, \quad (3)$$

where $p_{\bar{K}}$ and p_π are initial antikaon and final pion momenta in the center-of-mass system, and $|M_{\bar{K}\Lambda \rightarrow \pi\Xi}|^2$ and $|M_{\bar{K}\Sigma \rightarrow \pi\Xi}|^2$ are squared invariant matrix elements with summation over the spins and isospins of both initial and final particles. The results from the coupled-channel approach with cutoff parameter of 1 GeV can be fitted by using the following parameterization for the squared invariant matrix elements:

$$|M_{\bar{K}\Lambda \rightarrow \pi\Xi}|^2 = 34.7 \frac{s_0}{s} \text{ mb}, \quad |M_{\bar{K}\Sigma \rightarrow \pi\Xi}|^2 = 318 \left(1 - \frac{s_0}{s}\right)^{0.6} \left(\frac{s_0}{s}\right)^{1.7} \text{ mb} \quad (4)$$

where the threshold energy $s_0^{1/2}$ in the center-of mass system is 1.611 GeV and 1.688 GeV for the reactions $\bar{K}\Lambda \rightarrow \pi\Xi$ and $\bar{K}\Sigma \rightarrow \pi\Xi$, respectively. In Figs. 1(a) and (b), we show

by solid curves the cross sections for the two reactions $\bar{K}\Lambda \rightarrow \pi\Xi$ and $\bar{K}\Sigma \rightarrow \pi\Xi$ from the coupled-channel approach and by dashed curves those using the parameterizations of Eq.(4). Except near threshold, these cross sections are of the order of 5-10 mb.

The cross sections for the inverse reactions $\pi\Xi \rightarrow \bar{K}\Lambda$ and $\pi\Xi \rightarrow \bar{K}\Sigma$, which are needed for treating Ξ annihilation, are related to those for Ξ production by the principle of detailed balancing, i.e.,

$$\sigma_{\pi\Xi \rightarrow \bar{K}\Lambda} = \frac{1}{3} \frac{p_{\bar{K}}^2}{p_{\pi}^2} \sigma_{\bar{K}\Lambda \rightarrow \pi\Xi}, \quad \sigma_{\pi\Xi \rightarrow \bar{K}\Sigma} = \frac{p_{\bar{K}}^2}{p_{\pi}^2} \sigma_{\bar{K}\Sigma \rightarrow \pi\Xi}. \quad (5)$$

These cross sections are shown in Figs. 1(c) and (d) by solid curves for those from the coupled-channel approach and by dashed curves for the parameterized ones.

IV. KAON AND ANTIKAON DYNAMICS

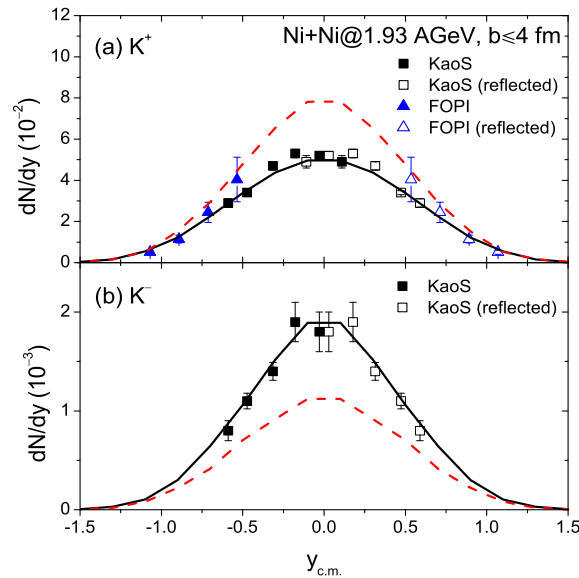


FIG. 2: Rapidity distributions of (a) K^+ and (b) K^- with (solid lines) and without (dashed lines) kaon medium effects in near-central collisions of $^{58}\text{Ni} + ^{58}\text{Ni}$ at $E/A = 1.93$ GeV. The experimental data are from the FOPI [23] and KaoS [24] collaborations.

Since the effective masses of kaons and antikaons are modified in nuclear medium, their production cross sections differ from those in free space. Following Refs.[11, 12], their values at center-of-mass energy $\sqrt{s^*} - \sqrt{s_{\text{threshold}}^*}$ above the threshold energy $\sqrt{s_{\text{threshold}}^*}$ in the medium are taken to have same values as those at center-of-mass energy $\sqrt{s} - \sqrt{s_{\text{threshold}}}$ above

the threshold energy $\sqrt{s_{\text{threshold}}}$ in free space. Taking into account also propagation of kaons and antikaons in their mean-field potentials given by Eq.(2), we have studied kaon and antikaon production in near-central collisions of $^{58}\text{Ni} + ^{58}\text{Ni}$ at $E/A = 1.93$ GeV. We find that the measured rapidity distributions of kaons and antikaons [23, 24], shown by squares in Figs. 2(a) and (b), respectively, can be fitted with the parameters $a_K = 0.22 \text{ GeV}^2\text{fm}^3$ and $a_{\bar{K}} = 0.35 \text{ GeV}^2\text{fm}^3$. These values are somewhat smaller than those used in Ref. [25] since slightly different cross sections are used in the present study as discussed in the previous section.

The above parameters give a repulsive potential of about 20 MeV for kaons and an attractive potential of about -98 MeV for antikaons with zero momentum in a nuclear matter at normal density. This value of kaon potential is consistent with that known empirically from the kaon-nucleus scattering [26] and also from a more recent study of soft kaon production in p+A reactions at COSY-Jülich [27]. The magnitude of the antikaon potential is smaller than that extracted from the kaonic atom data [28], which is about -200 ± 20 MeV but depends strongly on the extrapolation procedure from the surface of nuclei to their interiors [28]. It is, however, comparable to the moderate attractive potential with magnitude of about 50-90 MeV predicted by recent studies based on self-consistent calculations with a chiral Lagrangian [29, 30] or meson-exchange potentials [31]. The relatively shallow antikaon-nucleus potential has also been found to reproduce reasonably the experimental data on kaonic atoms in studies based on the SU(3) chiral unitary model [32]. The present values of kaon and antikaon potentials determined from fitting the experimental data on kaon and antikaon yield in heavy-ion collisions using the RVUU model are thus reasonable.

In Fig. 2, we also show the results from the RVUU model without kaon medium effects. It is seen that the repulsive kaon potential reduces kaon production due to the higher threshold while the attractive antikaon potential enhances antikaon production as a result of lower threshold. Including medium effects on kaon and antikaon production in heavy ion collisions are thus important in describing the measured kaon and antikaon yields.

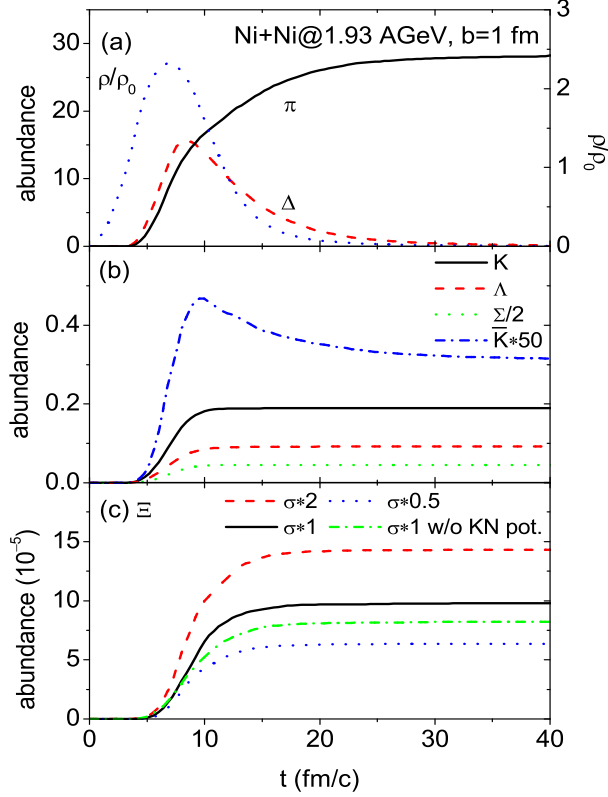


FIG. 3: Time evolutions of (a) central baryon density (right scales) and abundances (left scales) of π , Δ ; (b) abundances of K , Λ , Σ , and \bar{K} ; and (c) the Ξ abundance in cases with and without kaon medium effects and different cross sections (see text) in collisions of $^{58}\text{Ni} + ^{58}\text{Ni}$ at $E/A = 1.93$ GeV at $b = 1$ fm.

V. RESULTS

A. Nonstrange and singly strange hadrons

We first show in Fig. 3 the time evolutions of (a) central baryon density and the abundances of π , Δ , and (b) K , Λ , Σ , \bar{K} in collisions of $^{58}\text{Ni} + ^{58}\text{Ni}$ at energy $E/A = 1.93$ GeV and at impact parameter $b = 1$ fm. It is seen that the colliding system reaches the highest compression of central baryon density of about $2.3\rho_0$ at about 7 fm/c, and most particles are produced during this compression stage. The final π multiplicity is about 28, corresponding to an averaged charged pion multiplicity $(\pi^+ + \pi^-)/2$ of about 9.3, which is in good agreement with the experimental data [33]. The abundances of K , Λ , and Σ reach their respective final values of 0.189, 0.092, and 0.091 quickly at about 10 fm/c, while the \bar{K}

abundance first increases and then decreases to its final value of about 6.3×10^{-3} at around 30 fm/c. The decrease of the \bar{K} abundance is due to the strong \bar{K} absorption through the strangeness-exchange reactions $\bar{K}N \rightarrow \pi Y$. The final \bar{K}/K ratio is about 3.3×10^{-2} and is again in good agreement with experimental data and is also comparable to the predictions from the statistical model [34].

B. Ξ production from $^{58}\text{Ni} + ^{58}\text{Ni}$ collisions at $E/A = 1.93$ GeV

The time evolution of the Ξ abundance from this reaction is shown by the solid curve in Fig. 3(c). The Ξ abundance is seen to reach its final value of about 9.8×10^{-5} at about 20 fm/c. The resulting Ξ/K ratio is thus about 5.2×10^{-4} and is measurable in experiments at GSI. To see how the Ξ abundance depends on the cross sections for the strangeness-exchange reactions $\bar{K}\Lambda \leftrightarrow \pi\Xi$ and $\bar{K}\Sigma \leftrightarrow \pi\Xi$, we also show in Fig. 3 (c) the time evolution of the Ξ abundance from same heavy-ion collisions when the cross sections for the strangeness-exchange reactions are varied by a factor 2. This changes the Ξ abundance to 1.4×10^{-4} and 6.3×10^{-5} , corresponding to effects of about 46% and 36%, when the cross sections for the strangeness-exchange reactions are doubled (dashed line in Fig. 3 (c)) and halved (dotted line in Fig. 3 (c)). Our results thus show that the Ξ yield in heavy ion collisions does not reach chemical equilibrium, similar to the conclusion of Ref.[35] on subthreshold \bar{K} production in heavy-ion collisions at SIS energies.

In Fig. 3(c), we also show by the dash-dotted curve the Ξ abundance in the case of neglecting kaon medium effects. In this case, the final Ξ yield is about 8.2×10^{-5} and is only about 16% less than that from including kaon medium effects. The small effect is due to the fact that kaon medium effects increase the \bar{K} abundance but decrease the abundance of Λ and Σ . The Ξ abundance is thus more sensitive to the cross sections for strangeness-exchange reactions than to the medium effects due to the modification of kaon properties. Study of Ξ production in heavy-ion collisions at SIS energies thus provides the possibility to understand the strangeness-exchange reactions $\bar{K}\Lambda \leftrightarrow \pi\Xi$ and $\bar{K}\Sigma \leftrightarrow \pi\Xi$, and to test the hadronic model used in Ref.[8] for studying these reactions.

To see the centrality dependence of particle production, we show in Figs. 4(a) the abundances of K , \bar{K} , and Ξ , and (b) the \bar{K}/K and Ξ/K ratios as functions of impact parameter b in collisions of $^{58}\text{Ni} + ^{58}\text{Ni}$ at $E/A = 1.93$ GeV. It is seen that the abundances of K , \bar{K}

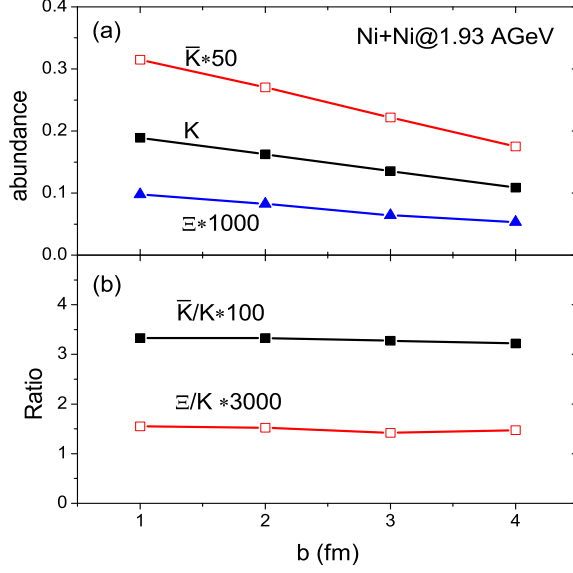


FIG. 4: (a) Abundances of K , \bar{K} , and Ξ , and (b) \bar{K}/K and Ξ/K ratios as functions of impact parameter b in collisions of $^{58}\text{Ni} + ^{58}\text{Ni}$ at $E/A = 1.93$ GeV.

and Ξ decrease almost linearly with b while the \bar{K}/K and Ξ/K ratios only depend weakly on centrality. For the \bar{K}/K ratio, its value is in the range $3.2 \times 10^{-2} \sim 3.3 \times 10^{-2}$ for impact parameters between 1 and 4 fm and agrees well with the experimental data [34]. The weak centrality dependence of \bar{K}/K was also observed in previous calculations [12]. The predicted variation of the Ξ/K ratio with impact parameter is in the range $4.7 \times 10^{-4} \sim 5.2 \times 10^{-4}$.

C. Ξ production from $^{197}\text{Au} + ^{197}\text{Au}$

It is also of interest to study Ξ production from other collision systems and at different energies. Shown in Fig. 5(a) are excitation functions for the abundances of K , \bar{K} , and Ξ from central collisions of $^{197}\text{Au} + ^{197}\text{Au}$ at $b = 1$ fm. The Ξ abundance is about 5.4×10^{-6} , 1.8×10^{-4} , and 9.6×10^{-4} at $E/A = 0.96$, 1.48, and 2.0 GeV, respectively. Therefore, the Ξ yield depends on the incident energy and mass of the colliding system. Figs. 5(b) shows the \bar{K}/K and Ξ/K ratios as functions of incident energy in collisions of $^{197}\text{Au} + ^{197}\text{Au}$ at $b = 1$ fm. It is seen that the \bar{K}/K and Ξ/K ratios increase with increasing incident energy. In particular, large Ξ abundance of about 1.0×10^{-3} and Ξ/K ratio of about 7.3×10^{-4} are obtained in central $^{197}\text{Au} + ^{197}\text{Au}$ collisions at $E/A = 2.0$ GeV, which can be studied at AGS [36, 37].

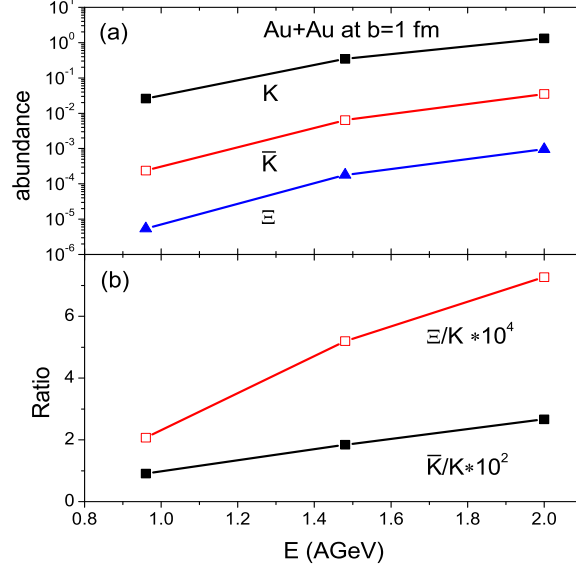


FIG. 5: Excitation functions for (a) the abundance of K , \bar{K} , and Ξ , and (b) \bar{K}/K and Ξ/K ratios from central collisions of $^{197}\text{Au} + ^{197}\text{Au}$ at $b = 1$ fm.

VI. SUMMARY

In summary, we have studied subthreshold Ξ production in heavy-ion collisions at SIS energies within the framework of a relativistic transport model that includes explicitly the nucleon, Δ , and pion, and perturbatively the kaon, antikaon, and hyperons. The production of Ξ is also treated perturbatively through the strangeness-exchange reactions $\bar{K}\Lambda \rightarrow \pi\Xi$ and $\bar{K}\Sigma \rightarrow \pi\Xi$ with their cross sections taken from the predictions from a hadronic model. We find that the Ξ yield is about 10^{-4} per event in central collisions of $^{58}\text{Ni} + ^{58}\text{Ni}$ at $E/A = 1.93$ GeV and can reach to about 10^{-3} per event in central collisions of $^{197}\text{Au} + ^{197}\text{Au}$ at $E/A = 2.0$ GeV. The Ξ yield is further found to be more sensitive to the cross sections for the strangeness-exchange reactions than to the kaon medium effects. Study of subthreshold Ξ production in heavy ion collisions at SIS energies thus provides the possibility of studying the strangeness-exchange reactions and testing the hadronic model used for evaluating their cross sections.

Acknowledgments

This paper was based on work supported by the U.S. National Science Foundation under Grant No. PHY-0098805 and the Welch Foundation under Grant No. A-1358. L.W.C. was also supported by the National Natural Science Foundation of China under Grant No. 10105008. Y.T. would like to express his gratitude to the Cyclotron Institute at TAMU for the warm hospitality during his visit, and his work was supported by Taiwan's National Science Council Grant NSC92-2112-M001-64

-
- [1] E. Anderson *et al.* (WA97 Collaboration), Phys. Lett. B **433**, 209 (1998); *ibid.* **449**, 401 (1999).
 - [2] S. Pal, C.M. Ko, and Z.W. Lin, Nucl. Phys. **A730**, 143 (2004).
 - [3] P. Chung *et al.* (E895 Collaboration), Phys. Rev. Lett. **91**, 202301 (2003).
 - [4] S. Pal, C.M. Ko, J. M. Alexander, P. Chung, and R.A. Lacey, arXiv:nucl-th/0211020.
 - [5] P. Braun-Munzinger, K. Redlich, and J. Stachel, nucl-th/0304013.
 - [6] C.M. Ko and G.Q. Li, J. Phys. G **22**, 1673 (1996).
 - [7] W. Cassing and E.L. Bratkovskaya, Phys. Rep. **308**, 65 (1999).
 - [8] C.H. Li and C.M. Ko, Nucl. Phys. **A712**, 110 (2002).
 - [9] G.Q. Li, C.M. Ko, and X.S. Fang, Phys. Lett. B **329**, 149 (1994).
 - [10] W. Cassing, E.L. Bratkovskaya, U. Mosel, S. Teis, and A. Sibirtsev, Nucl. Phys. **A614**, 415 (1997).
 - [11] G.Q. Li, C.H. Lee, and G.E. Brown, Nucl. Phys. **A625**, 372 (1997).
 - [12] G.Q. Li and G.E. Brown, Phys. Rev. C **58**, 1698 (1998); Nucl. Phys. **A636**, 487 (1998).
 - [13] C.M. Ko, Q. Li, and R. Wang, Phys. Rev. Lett. **59**, 1084 (1987); C.M. Ko and Q. Li, Phys. Rev. C **37**, 2270 (1988); Q. Li, J.Q. Wu, and C.M. Ko, *ibid.* **39**, 849 (1989); C.M. Ko, Nucl. Phys. **A495**, 321c (1989).
 - [14] R.J. Furnstahl, H.B. Tang, and B.D. Serot, Phys. Rev. C **52**, 1368 (1995).
 - [15] K. Tsushima, S.W. Huang, and A. Faessler, Phys. Lett. B **337**, 245 (1994); J. Phys. G **21**, 33 (1995).
 - [16] K. Tsushima, A. Sibirtsev, A. W. Thomas, and G. Q. Li, Phys. Rev. C **59**, 369 (1999), *ibid.*

- 61**, 029903(E) (2000).
- [17] G.Q. Li and C.M. Ko, Nucl. Phys. **A594**, 439 (1995).
 - [18] G.Q. Li, C.M. Ko, and W.S. Chung, Phys. Rev. C **57**, 434 (1998).
 - [19] C.M. Ko, Phys. Lett. B **120**, 294 (1983).
 - [20] S. Pal, C.M. Ko, and Z.W. Lin, Phys. Rev. C **64**, 042201 (2001).
 - [21] C.H. Lee, G.E. Brown, D.P. Min, and M. Rho, Nucl. Phys. **A585** 401 (1995).
 - [22] R. Randrup and C.M. Ko, Nucl. Phys. **A343**, 519 (1980).
 - [23] D. Best *et al.* (FOPI Collaboration), Nucl. Phys. **A625**, 307 (1997).
 - [24] M. Menzel *et al.* (KaoS Collaboration), Phys. Lett. B **495**, 26 (2000).
 - [25] G. Q. Li, C.-H. Lee, and G. E. Brown, Phys. Rev. Lett. **79**, 5214 (1997).
 - [26] T. Barnes and E.S. Swanson, Phys. Rev. C **49** 1166 (1994).
 - [27] M. Nikipelov *et al.*, Phys. Lett. B **540**, 207 (2002).
 - [28] E. Friedman, A. Gal, and C.J. Batty, Phys. Lett. B **308**, 6 (1993); Nucl. Phys. **A579**, 518 (1994).
 - [29] M. Lutz, Phys. Lett. B **426**, 12 (1998).
 - [30] A. Ramos and E. Oset, Nucl. Phys. **A671**, 481 (2000).
 - [31] L. Tolós, A. Ramos, A. Polls, and T. T. S. Kuo, Nucl. Phys. **A690**, 547 (2001).
 - [32] S. Hirenzaki, Y. Okumura, H. Toki, E. Oset, and A. Ramos, Phys. Rev. C **61** 055205 (2000).
 - [33] D. Pelte *et al.* (FOPI collaboration), Z. Phys. A **359**, 55 (1997).
 - [34] H. Oeschler, J. Phys. G **27**, 257 (2001).
 - [35] Ch. Hartnack, H. Oeschler, and J. Aichelin, Phys. Rev. Lett. **90**, 102302 (2003).
 - [36] L. Ahel *et al.* (E866 Collaboration) and B.B. Back *et al.* (E917 Collaboration), Phys. Lett. B **476**, 1 (2000).
 - [37] P. Chung *et al.* (E895 Collaboration), Phys. Rev. C **66**, 021901(R) (2002).